EUR 572.e
REPRINT

EUROPEAN ATOMIC ENERGY COMMUNITY - EURATOM

A DEVICE FOR COUPLING A PULSE HEIGHT DISCRIMINATOR TO A SCANNING X-RAY SPECTROMETER

by

K. WEBER and J. MARCHAL

1964

Joint Nuclear Research Center
Ispra Establishment - Italy
Materials Department

Reprinted from
JOURNAL OF SCIENTIFIC INSTRUMENTS
Vol. 41 - 1964

LEGAL NOTICE

This document was prepared under the sponsorship of the Commission of the European Atomic Energy Community (EURATOM).

Neither the EURATOM Commission, its contractors nor any person acting on their behalf:

1° — Make any warranty or representation, express or implied, with respect to the accuracy, completeness, or usefulness of the information contained in this document, or that the use of any information, apparatus, method, or process disclosed in this document may not infringe privately owned rights; or

2° — Assume any liability with respect to the use of, or for damages resulting from the use of any information, apparatus, method or process disclosed in this document.

This reprint is intended for restricted distribution only. It reproduces, by kind permission of the publisher, an article from "JOURNAL OF SCIENTIFIC INSTRUMENTS", Vol. 41 - 1964, 15-22. For further copies please apply to The Institute of Physics and the Physical Society — 1 Lowther Gardens - Prince Consort Road, London S.W.7 (England).

Dieser Sonderdruck ist für eine beschränkte Verteilung bestimmt. Die Wiedergabe des vorliegenden in „JOURNAL OF SCIENTIFIC INSTRUMENTS", Vol. 41 - 1964, 15-22 erschienenen Aufsatzes erfolgt mit freundlicher Genehmigung des Herausgebers. Bestellungen weiterer Exemplare sind an The Institute of Physics and the Physical Society — 1 Lowther Gardens - Prince Consort Road, London S.W. 7 (England), zu richten.

Ce tiré-à-part est exclusivement destiné à une diffusion restreinte. Il reprend, avec l'aimable autorisation de l'éditeur, un article publié dans le « *JOURNAL OF SCIENTIFIC INSTRUMENTS* », *Vol. 41 - 1964, 15-22. Tout autre exemplaire de cet article doit être demandé à The Institute of Physics and the Physical Society — 1 Lowther Gardens - Prince Consort Road, London S.W. 7 (England).*

Questo estratto è destinato esclusivamente ad una diffusione limitata. Esso è stato riprodotto, per gentile concessione dell'Editore, da « *JOURNAL OF SCIENTIFIC INSTRUMENTS* », *Vol. 41 - 1964, 15-22. Ulteriori copie dell'articolo debbono essere richieste a The Institute of Physics and the Physical Society — 1 Lowther Gardens - Prince Consort Road, London S.W. 7 (England).*

Deze overdruk is slechts voor beperkte verspreiding bestemd. Het artikel is met welwillende toestemming van de uitgever overgenomen uit „JOURNAL OF SCIENTIFIC INSTRUMENTS", Vol. 41 - 1964, 15-22. Meer exemplaren kunnen besteld worden bij The Institute of Physics and the Physical Society — 1 Lowther Gardens - Prince Consort Road, London S.W. 7 (England).

EUR 572.e

REPRINT

A DEVICE FOR COUPLING A PULSE HEIGHT DISCRIMINATOR TO A SCANNING X-RAY SPECTROMETER by K. WEBER and J. MARCHAL.

European Atomic Energy Community - EURATOM.
Joint Nuclear Research Center.
Ispra Establishment (Italy).
Materials Department.
Mineralogy and Geochemistry Section.
Reprinted from "Journal of Scientific Instruments", Vol. 41 - 1964, pages 15-22.

A simple control device has been developed to synchronize a single-channel pulse height discriminator with the rotation of the crystal in an x-ray spectrometer over an energy range of 1 : 8. Both the bias voltage and the window width of the discriminator are continuously adjusted. The spectrometer had a 50 kv tungsten target x-ray tube, an LiF analysing crystal and a scintillation counter. With this arrangement the line-to-background ratio for a wavelenght of about 2·8 Å is improved by a factor of 33 compared with results obtained without a discriminator. Second-order reflections were attenuated within the whole waveband $0{\cdot}35 < \lambda > 2{\cdot}8$ Å by a factor of at least 60, and third-order reflections by a factor of at least 400.

EUR 572.e

REPRINT

A DEVICE FOR COUPLING A PULSE HEIGHT DISCRIMINATOR TO A SCANNING X-RAY SPECTROMETER by K. WEBER and J. MARCHAL.

European Atomic Energy Community - EURATOM.
Joint Nuclear Research Center.
Ispra Establishment (Italy).
Materials Department.
Mineralogy and Geochemistry Section.
Reprinted from "Journal of Scientific Instruments", Vol. 41 - 1964, pages 15-22.

A simple control device has been developed to synchronize a single-channel pulse height discriminator with the rotation of the crystal in an x-ray spectrometer over an energy range of 1 : 8. Both the bias voltage and the window width of the discriminator are continuously adjusted. The spectrometer had a 50 kv tungsten target x-ray tube, an LiF analysing crystal and a scintillation counter. With this arrangement the line-to-background ratio for a wavelenght of about 2·8 Å is improved by a factor of 33 compared with results obtained without a discriminator. Second-order reflections were attenuated within the whole waveband $0{\cdot}35 < \lambda > 2{\cdot}8$ Å by a factor of at least 60, and third-order reflections by a factor of at least 400.

EUR 572.e

REPRINT

A DEVICE FOR COUPLING A PULSE HEIGHT DISCRIMINATOR TO A SCANNING X-RAY SPECTROMETER by K. WEBER and J. MARCHAL.

European Atomic Energy Community - EURATOM.
Joint Nuclear Research Center.
Ispra Establishment (Italy).
Materials Department.
Mineralogy and Geochemistry Section.
Reprinted from "Journal of Scientific Instruments", Vol. 41 - 1964, pages 15-22.

A simple control device has been developed to synchronize a single-channel pulse height discriminator with the rotation of the crystal in an x-ray spectrometer over an energy range of 1 : 8. Both the bias voltage and the window width of the discriminator are continuously adjusted. The spectrometer had a 50 kv tungsten target x-ray tube, an LiF analysing crystal and a scintillation counter. With this arrangement the line-to-background ratio for a wavelenght of about 2·8 Å is improved by a factor of 33 compared with results obtained without a discriminator. Second-order reflections were attenuated within the whole waveband $0{\cdot}35 < \lambda > 2{\cdot}8$ Å by a factor of at least 60, and third-order reflections by a factor of at least 400.

Reprinted from the *Journal of Scientific Instruments*, VOL. 41, pp. 15–22, JANUARY 1964

A device for coupling a pulse height discriminator to a scanning X-ray spectrometer

K. WEBER and J. MARCHAL
European Atomic Energy Community, Euratom CCR Ispra, Italy
MS. received 16*th April* 1963, *and in revised form* 10*th September* 1963

Abstract. A simple control device has been developed to synchronize a single-channel pulse height discriminator with the rotation of the crystal in an x-ray spectrometer over an energy range of 1 : 8. Both the bias voltage and the window width of the discriminator are continuously adjusted. The spectrometer had a 50 kv tungsten target x-ray tube, an LiF analysing crystal and a scintillation counter. With this arrangement the line-to-background ratio for a wavelength of about 2·8 Å is improved by a factor of 33 compared with results obtained without a discriminator. Second-order reflections were attenuated within the whole waveband $0{\cdot}35 < \lambda > 2{\cdot}8$ Å by a factor of at least 60, and third-order reflections by a factor of at least 400.

1. Introduction

Considerable experience in the x-ray fluorescence analysis of mineral and rock specimens, in which many elements occur simultaneously and sometimes unexpectedly, have led us to the development of the device described here. The advantage of the extension of pulse height discrimination over the whole registered spectrum is well known (see, for example, Heinrich 1961): both the accuracy of measurement of minor constituents† and the detection limit in recordings of spectra are considerably improved. With exception of the work of Philips (see *Chem. Weekbl.* 1962) no practical application seems to be known and this encouraged us to publish our method, which is easy to put into practice and not expensive. This type of discrimination could also be used for micro-probe analysers in trace analysis.

2. General considerations

The principal parts of an x-ray spectrometer for analytical purposes are: (i) an electron beam or an x-ray source for stimulating the x-ray spectrum of the specimen under examination, (ii) a spectrometer arrangement, in general a single crystal spectrometer, to analyse the specimen spectrum into its several wavelengths λ, and (iii) the detector unit. In the Bragg type spectrometer used here a (plane) analysing crystal turns uniformly about its axis and so continuously changes the angle of incidence θ. According to Bragg's equation $n\lambda = 2d \sin\theta$ the wavelength λ is reflected in nth order for an angle of incidence θ (d = interplanar spacing of the analysing crystal). The usual detector for the region $\lambda < 3$ Å is a scintillation counter, which is used because of its constant quantum sensitivity over a wide range of λ, a short resolution time compared with that of Geiger counters, and the fact that the amplitude of the output pulse is proportional to the energy E of the incident photon

$$E = hc/\lambda \qquad (1)$$

where h = Planck's constant and c = velocity of light. The last-mentioned property, which is common also to gas-filled proportional counters, makes it possible to separate superpositions of spectral lines or scattered radiations of different reflection orders n corresponding to their different energies nE. Therefore, the spectrograph has a proportional amplifier and a single channel discriminator to regulate electronically the passage of the wanted quantum energy E corresponding to wavelength λ. The standard deviation of the pulse height distribution on the output of the scintillation counter decreases as $E^{1/2}$; consequently, the required relative channel width of the discriminator is also a function of E.

For any fixed value of θ it is necessary to adjust both (*a*) the mean quantum energy passage and (*b*) the channel width; for scanning through a spectrum it is necessary to synchronize the corresponding electronic circuits (*a*) and (*b*) with the angle of incidence.

The electronic circuit (*a*), if linear, has to satisfy a relation of the following kind:

$$V_d \propto EMM_p \qquad (2)$$

where V_d is the mean discriminator threshold voltage (in volts), M is the amplification factor of the circuit, including preamplifier, cathode follower and linear amplifier, M_p the gain of the photomultiplier, which varies as a high power ($\sim$7) of V_h (Birks 1960), and V_h is the total voltage at the photomultiplier.

Coupling this circuit with the angle of incidence θ, by combining (1) and (2) with the Bragg equation, we find

$$\text{const.} \times \sin\theta = MM_p/V_d. \qquad (3)$$

With the variables M, V_d and M_p, there are basically three different possibilities of synchronization. While in the new Philips apparatus the amplification factor M is varied, we have selected the condition

$$V_d = \text{const.}/\sin\theta$$

V_h and M being both kept constant, because from our point

† Major constituents, i.e. high pulse rates, generally reduce the accuracy of measurements when one is operating with a discriminator. However, in such cases one can easily find devices to short circuit the discriminator automatically.

of view, it seems the simplest.† Furthermore, it has good stability and covers the whole working range of θ. Finally it is possible to register the spectra in the second, third and higher orders by replacing the values M of the linear amplifier by $M/2$, $M/3$ and so on, according to equation (2), without changing the discriminator. The circuit can be adapted in the same manner to another analysing crystal by multiplying M by the ratio of the d values of the two corresponding analysing crystals.

With an LiF crystal ($2d = 4{\cdot}028$ Å) the K or L spectra of all elements from Ti up to the end of the periodic system are reflected within the range of angle of incidence θ from 5° to 45°. In this case the discrimination curve $V_d(\theta)$ extends over a range of energy of a little more than 1 : 8. In principle $V_d(\theta)$ could be represented by a potentiometer with a cosecant characteristic, coupled with the θ axis. Apart from other disadvantages of this arrangement‡ equation (2) is not exactly fulfilled over an amplitude range of 1 : 8 (table 1) and it is better to construct a function generator on the basis of equation (4):

$$\frac{1}{\sin\theta} = \frac{1}{\theta} + \frac{\theta}{6} + \frac{7\theta^3}{360} + \ldots . \qquad (4)$$

The expansion into powers of θ allows a separate electrical adjustment of each term, and therefore allows the adaptation of the function generator to the individual $V_d(\theta)$ curve. In the above θ range, $1/\sin\theta$ can be well approximated by the first two terms of the series (4) only, as is shown in figure 1.

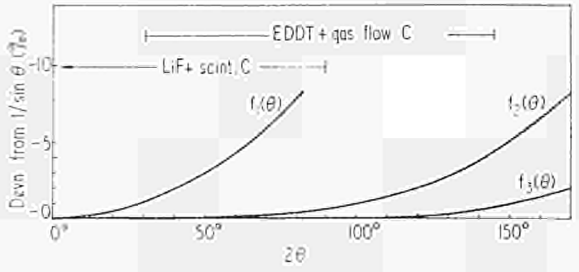

Figure 1. Divergence of the expansion into series (4) of the function $1/\sin\theta$ for different approximation states f_i; $f_1 = 1/\theta$, $f_2 = f_1 + \theta/6$, $f_3 = f_2 + 7\theta^3/360$.

As V_d is varied the required channel width is proportional to $(1/\sin\theta)^{1/2}$. Figure 4 shows that a linear change of the channel width with θ is completely sufficient. Therefore only linear potentiometers are needed in the circuit (*b*).

3. The device of control

One of the possible controlling devices for the discriminator threshold, using the first two terms of equation (4), is shown in figure 2. The linear potentiometers P1 and P2 produce respectively the hyperbolic and the linear term of the series (4). The axes of the potentiometers are coupled directly to the θ axis of the spectrometer by means of gears. The two potentiometers run in opposite directions. The ratio of the resistance R to $dP1/d\theta$ in figure 2 and the zero point of the resistance of P1 determine the hyperbola. In practice these values are not critical and the method could also be adapted—with even more advantage—for use in transistorized discriminators. In this case of course, the voltage stabilizer G1 should be replaced by a Zener diode.

The control device§ used for the Philips discriminator PW4082 with a channel width set symmetrically about the threshold voltage is shown in figure 3. This discriminator works from about 5 v to 100 v. P1 consists of two three-turn

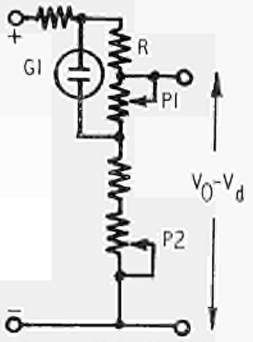

Figure 2. Basic circuit of the function generator to simulate $1/\sin\theta$.

helipots, each of 100 kΩ, in series. P1 is coupled with the θ axis by a reducing gear of 12 : 1. P2 is omitted; the function of P2 is taken over approximately by the resistances R1, which compensate the different operating voltage of the

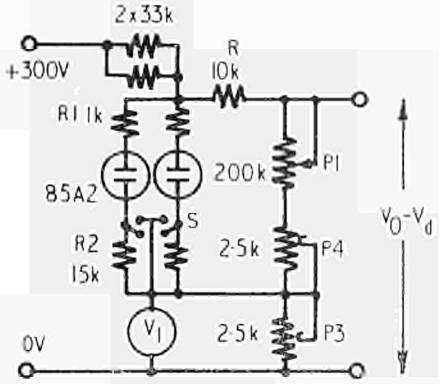

Fig. 3. The control device for the Philips discriminator PW4082.

stabilizers 85A2. The resistances R2 serve only for ignition of 85A2 and during operation are short-circuited by S. P3 and P4 serve for adjustment at large and small angles of incidence θ respectively. Thus, we find in the circuit described above $V_d \sim 7{\cdot}2/\sin\theta$ (in volts).

For changing the channel width we have chosen the circuit shown in the upper part of figure 4. The experimental measurements of the half-width of the pulse height distribution curve for different values of λ have been found to be proportional to $E^{1/2}$. To change the channel width linearly, the two three-turn helipots of 30 kΩ of the circuit (*b*) are coupled with the θ axis on the same 12 : 1

† Since this paper was written Riggs (1963), using the same conditions, has published a device to facilitate a continuous θ adjustment of V_d by hand. See also Lang (1954).

‡ The required precise synchronization of a non-linear potentiometer with the goniometer θ axis complicates the mechanics. In the device described here only linear potentiometers are used; these can be adjusted independently on the θ axis and their resistance function can be determined more exactly than that of special potentiometers. There is also the advantage that they are cheaper and delivered more speedily.

§ A detailed description, including the mechanics, can be obtained from Weber, Bouvelle and Marchal (1963).

reduction gear. With the decrease of θ, the two potentiometers, running in opposite directions, symmetrically open the channel towards the top and bottom with respect to the

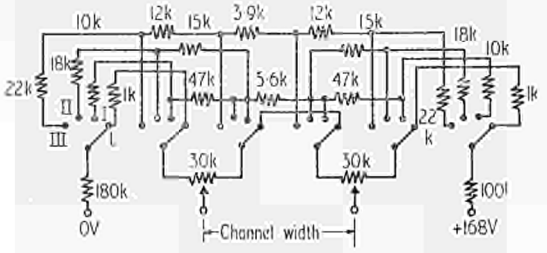

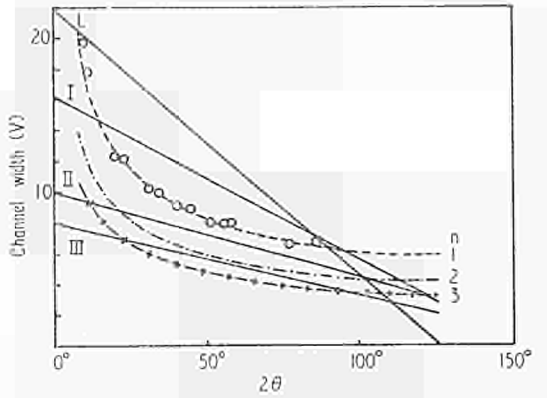

Figure 4. The channel-width circuit furnishes four channel-width functions, L, I, II and III, drawn in the graph. This shows the experimental half-width (circles show experimental points) of the pulses of the first-order reflections $n = 1$ in comparison with the approximation function $5{\cdot}45\ (n \sin\theta)^{-1/2}$ volts (broken line). The curves for $n = 2$ and $n = 3$ are calculated.

threshold voltage V_d. The circuit (*b*) furnishes four channel-width functions corresponding to the switch positions L, I, II and III. The four linear functions, drawn in the graph of figure 4, are adapted to the first (L and I), to the second (II) and to higher (III) order reflections.

4. Calibration control

Initial adaptation of the pulse heights to the automatic function $V_d(\theta) = 7{\cdot}2/\sin\theta$ is carried out by variation of the counter voltage V_h, until the mean experimental value $\overline{V'_d\lambda}$ (table 1) corresponds to the value $7{\cdot}2 \times 2d = 29{\cdot}0$ v Å.

Then the circuit (*a*) can be adjusted with P3 and P4 on two widely different angles of incidence. Away from the two calibration points there are small divergences between the automatic discriminator voltage V'_d and the wanted value V'_d. The deviations $V''_d - V'_d$ can be ascertained, at a fixed value of θ, by determining the pulse rate maximum on the discriminator output by varying V_1 by means of the adjusting potentiometer P3. The results are plotted in figure 5. The measured deviations are represented by the full line. The

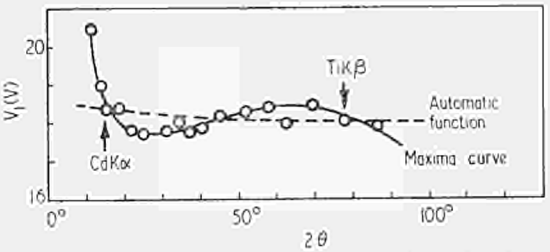

Figure 5. Experimental (– – –) and ideal (———) values of the voltage V_1 measured across the potentiometer P3.

broken line shows V_1 as a function of θ for automatic discrimination, i.e. when P3 is fixed. The difference of the two curves represents $V_d - V'_d$ in volts. In figure 5 the control device is adjusted on the pair of lines CdKα : TiKβ, which were found to be the most favourable. Using other calibration points, the agreement is not as good, as shown by the example BaKα : FeKα in figure 6. By comparing the curves of figure 6 with the values Δ of table 1, it is seen that

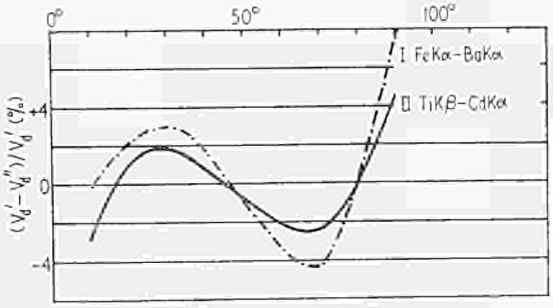

Figure 6. Dependence of $V'_d - V''_d$ on the choice of the pair of calibration points.

the function generator described here is able to compensate a great deal of the original non-linearities of ±5%. It may be mentioned that the essential part of the non-linearity of the circuit already exists at the input of the linear amplifier and is not attributed to the discriminator.

Initial adjustment of the channel potentiometers is carried out most simply at its zero point at $2\theta = 128°$ corresponding to a zero channel width for channel L (figure 4).

5. Measurements and results

With a 50 kv tungsten target tube, LiF crystal and scintillation counter at $2\theta = 90°$ a 33 : 1 improvement of the pulse-to-background ratio was obtained. This was gained by

Table 1. Experimental values V'_d of V_d, measured at low integral pulse rates (≈500 sec^{-1})

standard deviation ~ ±0·5%; channel width 1 volt; the maximum position of V'_d is found by assumption of a Gaussian curve. The values $\Delta = 100\{V'_d\lambda\,(V'_d\lambda)^{-1} - 1\}$ represent the non-linearity of the circuit.

Line	CaKα$_1$	CaKβ$_1$	TiKα$_1$	TiKβ$_1$	FeKα$_1$	FeKβ$_1$	CuKα$_1$	CuKβ$_1$
Energy (kev)†	3·69	4·01	4·51	4·93	6·40	7·06	8·05	8·90
V'_d (v)	8·4	9·3	10·4	11·2	15·0	16·8	19·3	21·7
Δ (%)	−1·6	+0·3	−0·3	−1·7	+1·3	+2·9	+3·7	+5·4
Line	**AsKα$_1$**	**AsKβ$_1$**	**ZrKα$_1$**	**ZrKβ$_1$**	**AgKα$_1$**	**AgKβ$_1$**	**BaKα$_1$**	**BaKβ$_1$**
Energy (kev)†	10·54	11·73	15·77	17·67	22·16	24·94	32·19	36·38
V'_d (v)	25·2	27·8	36·6	40·8	50·0	55·4	70·7	80·7
Δ (%)	+3·4	+2·5	+0·4	−0·2	−2·5	−4·0	−5·1	−4·1

† After Blochin (1957).

suppression of scattered radiation and noise outside the spectral order $n = 1$; this ratio at first decreases rapidly with decreasing θ and then more slowly (figure 7). The

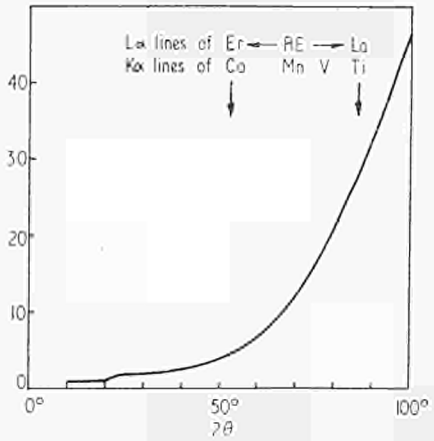

Figure 7. Improvement by the automatic discriminator of the line-to-background ratio. Arrangement: vacuum spectrometer, W-tube 50 kv, 18 mA; scintillation counter PW1964, LiF analysing crystal, primary collimator 160 μm/10 cm, secondary collimator 300 μm/4 cm. (RE represents rare earths region.)

attenuation ratios of the second- and third-order reflections are not constant, principally because of the different pulse height distributions and the different channel width. Second-order reflections are suppressed over the whole spectral range at least by a factor of 60, third-order reflections by a factor between 400 (Rb) and 2000 (Ba).

An alteration of the stabilizer voltage of about $\pm 0{\cdot}5\%$ does not change the registered pulse rate by more than $\pm 2\%$ within the most unfavourable range. The sign of the change, however, is different for the different ranges of θ (figure 5). The control device has been tested for more than six months with no detectable drift.

Figure 8 shows a complicated, but not unusual, spectral diagram of a uranium mineral specimen taken with the automatic discriminator in operation. Especially for large angles of incidence, the diagrams are considerably simplified and it is possible to work at a more sensitive scale factor of the recorder unit without need to change the speed. For instance, from figure 8(*c*) it is possible to estimate that a samarium content of 50 parts per million is still visible in a matrix like the present one. To facilitate the interpretation of the diagrams, peaks exceeding the intensity range of the recorder are registered by means of an inverting device which doubles the recorder scale. The process is as follows: at the end of the initial run the recorder pen inverts the direction of recording by operating a microswitch. This microswitch displaces the zero point of the recorder from left to right symmetrically with respect to the maximum position and so changes the recording direction. Thus the pen, moving in the opposite direction, brings the tops of the peaks back on to the diagram. In this way, it is easy to ascertain asymmetries of strong lines and therefore to detect superimposed lines: this is shown very clearly by the two lines TiKβ + VKα in figure 8(*c*) and also by the lines FeKβ + CoKα in figure 9. This device is only of value with automatic discrimination, as otherwise the higher orders would make the diagrams too complex to be usable.

To demonstrate the superpositions of different spectral orders n and the effectiveness of the device, we have recorded a specimen spectrum at the four amplification factors $M = 1$, $\frac{1}{2}$, $\frac{1}{3}$ and $\frac{1}{4}$ using the corresponding channel widths I, II and III respectively (figure 9). The different reflection orders can be simply identified by the different θ-values of the onset of the continuous radiation. Many superpositions are visibly separated by discrimination; for instance: $Ca_1K\beta + Cu_2K\alpha_2$, $CeL\alpha + W_2L\beta_1$, $Ce_1L\beta_1 + Zr_3K\alpha_2$, $Nd_1L\alpha + Zr_3K\alpha_1$, $Ni_1K\alpha + (Rb_2K\beta + Y_2K\alpha)$. Because the photon energy distance diminishes between neighbouring orders when n is increased, the discriminator is more effective between $n = 1$ and $n = 2$ than between $n = 2$ and $n = 3$. In the second-order diagram the residual values of the weaker lines of the first-order spectrum of Ca and Ti can be easily eliminated by operating the spectrometer without a vacuum. Only the very strong FeKα line is to be seen up to the fourth order. This is partially caused by 'piling up' of the pulses at higher pulse rates, which is explained later. Iron is a main constituent in the rocks and gives pulse rates of about $6 \times 10^4\,\mathrm{sec}^{-1}$. In trace analysis some corrections are needed for Cr, Mn, Fe, Ni, Cu, Zn and Pb, because the lines of these elements cause small contaminations of the primary x-ray beam.

The high sensitivity of the automatic discriminator makes necessary special attention to additional sources of error. One of these, which we have studied, is caused by the escape peaks. This kind of peak appears at the NaI-scintillation crystal, when the quantum energy E_i of the incident x-ray is higher than the binding energy E_k of the K electrons in iodine: $E_k = 33{\cdot}2$ kev, $\lambda_k = 0{\cdot}374$ Å (West *et al.* 1951). In this case an iodine fluorescence quantum E_f, generated with a certain probability during the absorption processes of the incident quantum E_i, can escape from the front face of the scintillation crystal, and the pulse height at the output of the photomultiplier is proportional to the energy difference $E_e = E_i - E_f$ only. Besides the normal peak at E_i, the pulse height distribution curve shows a satellite peak at E_e.

In scanning through a first-order spectrum, the detector passes positions θ_n of the nth order reflections which are not generally registered because the corresponding threshold value of the discriminator, being in the lower energy position E_i/n, blocks the passage of the quantum pulse height E_i. But it may be possible that the lower energy escape peak E_e can now pass the channel and so a line is registered in the spectral diagram. By trace analysis of barytes for example we have found two weak BaKβ-escape lines at 0·999 Å and at 1·363 Å. The first coincides approximately with the SeKβ-line (0·992 Å). Since the SeKα-line is covered by the diffused W-spectrum of the x-ray tube, it could be possible to misinterpret this line; however, in the above case the presence of selenium ($\sim$100 p.p.m. corresponding to the measured intensity) was hardly probable from the geological point of view.

Working with a 50 kv x-ray tube, we find that there are only four elements which give rise to escape lines: Cs, Ba, La and Ce. Elements with $Z > 59$ are excited with relatively small intensities and there is little probability that the spectral diagrams will be disturbed. We have measured the positions, the half-widths (table 2) and the relative intensities of several escape peaks within the range $33{\cdot}4\ \mathrm{kev} < E_i < 40{\cdot}1\ \mathrm{kev}$. The ratio R of the integrated intensity of the escape peak to that of the original peak is found to be about $\frac{1}{5}$ to $\frac{1}{4}$. This is a little smaller than the values calculated by Axel (1954) and found by Meyerhof and West (1955). The low accuracy of $\pm 20\%$ of our measurements gave no possibility of verifying the relation between R and E_i. With the data of table 2, it is possible to estimate the occurrence of escape lines at the positions of the different

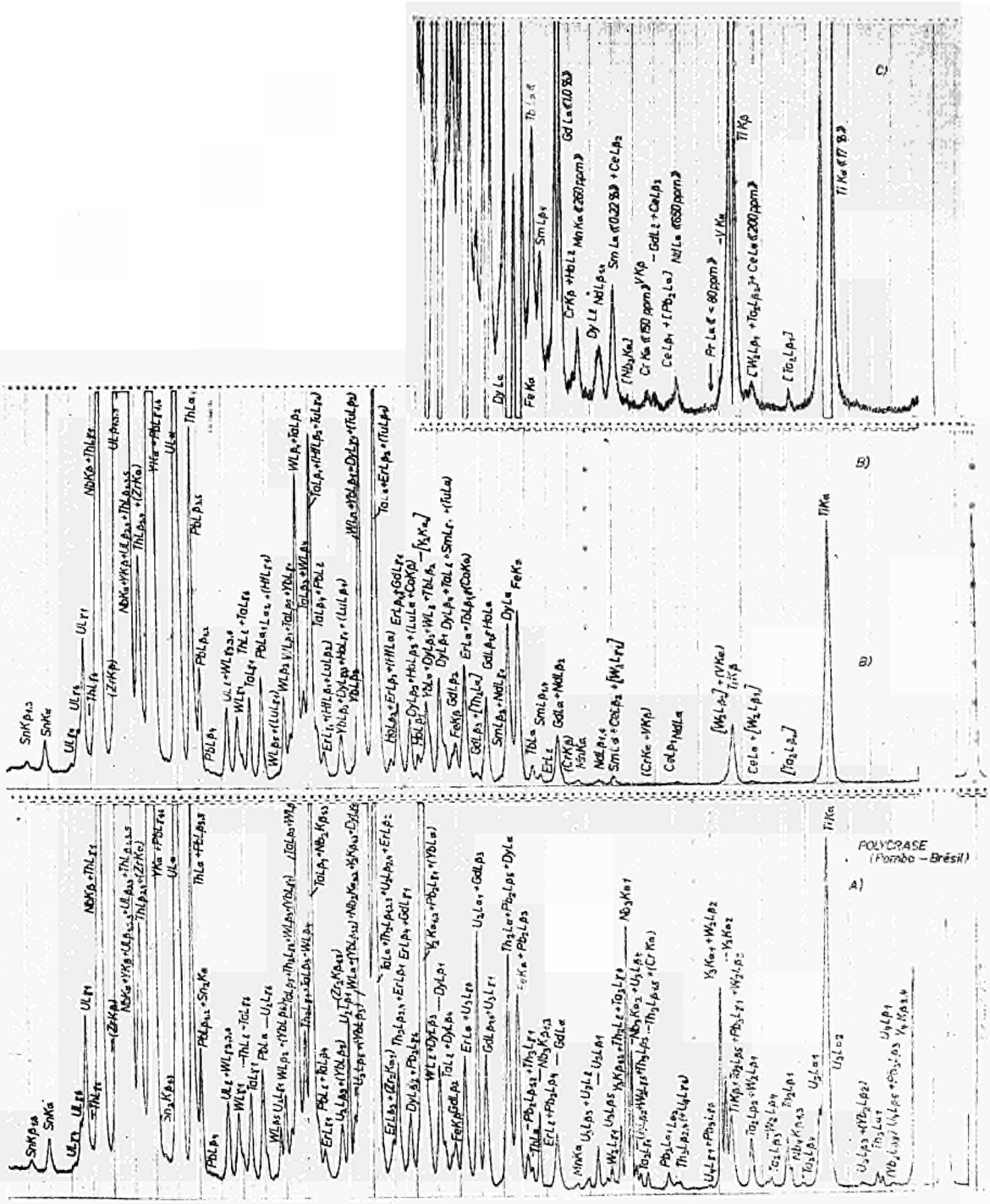

Figure 8. Spectral diagram of a mineral specimen taken (*A*) without (*B*) with the automatic discriminator. The partial diagram (*C*) is taken with a 16-fold higher sensitivity. The concentrations, determined chemically, of some elements, are given in brackets ⩽ ⩾. The recording speed of the three diagrams was 1° per min for the 2*θ*-circle; conditions as in figure 7.

Table 2. Escape peaks for NaI(Tl) crystals, measured with a 50 kV tungsten target X-ray tube

Original line		Escape peak				Escape line†			
	E_i (kev)	V_d (v)	E_e (kev)	half-width (%)	E_f (kev)	$n=2$	3	4	5
$LaK\alpha_1$	33·4	11·3 ± 5	5·0	60	28·4	o	o	−	+
$CeK\alpha_1$	34·7	14·2 ± 3	6·2	55	28·5	o	o	+	+
$BaK\beta_1$	36·3	18·0 ± 5	7·5	50	28·8	o	−	+	+
$LaK\beta_1$	37·8	22·6 ± 4	9·3	45	28·5	o	+	+	+
$CeK\beta_1$	39·2	25·5 ± 4	10·6	45	28·6	o	+	+	−
$CeK\beta_2$	40·1	26·7 ± 5	11·1	40	29·0	o	+	+	−
					mean 28·6 kev				

+, the maximum of the escape peak lies within the channel width; intensity >50%; −, the half width lies within the channel width; intensity >12%; o, intensity <12%.

† Occurrence of the escape line by scanning through a first-order spectrum in the position of the nth order original line.

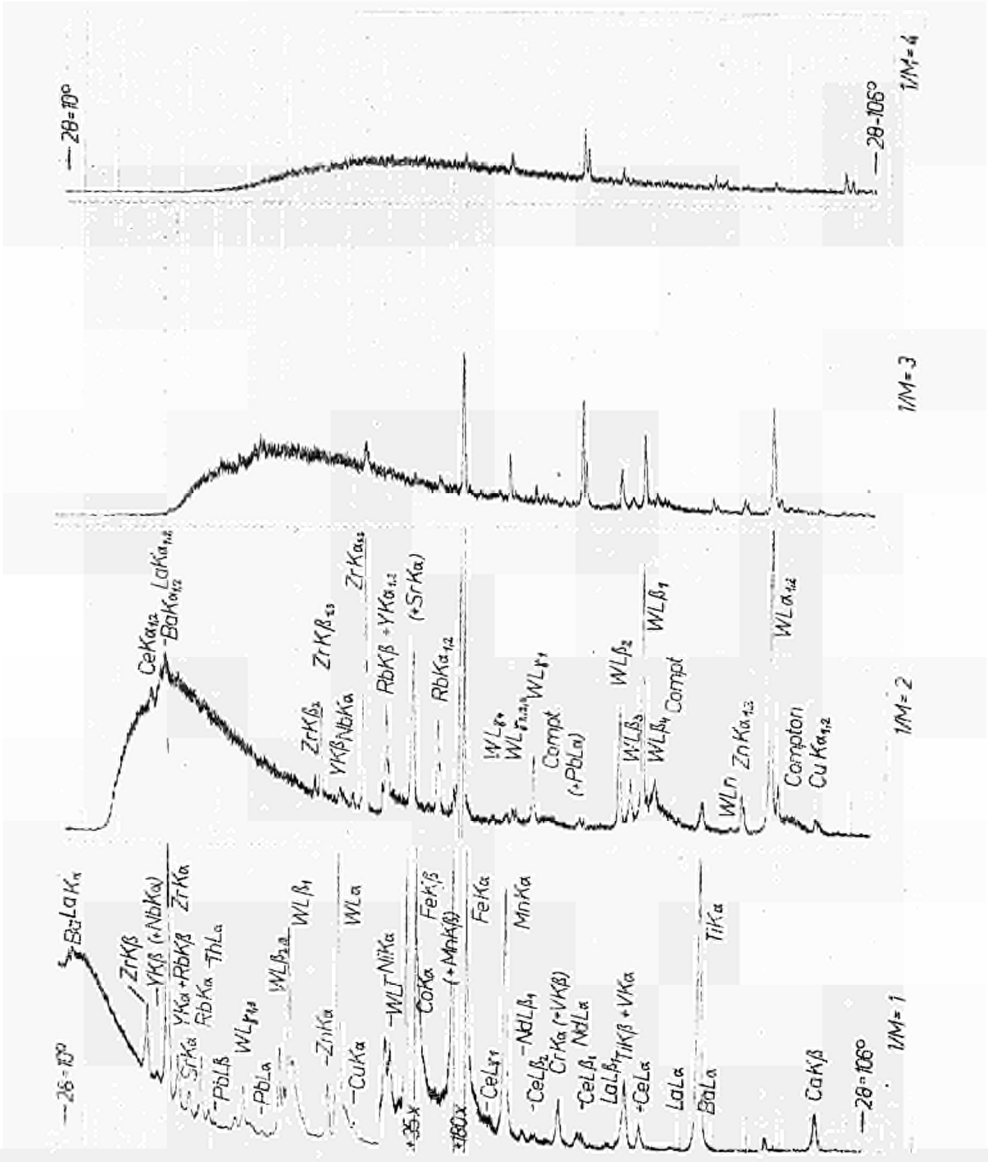

Figure 9. Different reflection orders of the spectral diagram of a soil specimen corresponding to different amplification factors M of the linear amplifier. Conditions as in figure 7; recording speed 1° per min; scale 500 sec^{-1} for $2\theta > 48°$; in the first- and second-order diagram the scale factor is changed at $2\theta = 48°$ by a factor of 4 and 2 respectively. Some element concentrations of this specimen are: Ca(1·6%), Ti(0·5%), La(100 p.p.m.), Cr(120 p.p.m.), Fe(5·5%), Co(40 p.p.m.), Cu(30 p.p.m.), Pb(40 p.p.m.), Th(160 p.p.m.), Rb(250 p.p.m.), Sr(20 p.p.m.), Zr(0·1%) and Nb(9 p.p.m.).

reflection orders of the original lines. We have added such values to the right-hand side of table 2 for the case of scanning a first-order spectrum.

When the operating voltage of the x-ray tube exceeds 50 kv, the intensities of the spectral lines of elements with $Z > 59$ increase rapidly; simultaneously the number of escape peaks rises and may complicate the spectral diagrams. For a series of elements, the increasing intensity of the original lines compensates the exponential decrease of $R_{(E_i - E_k)}$. However, there is a quick test to identify escape lines: if we filter the x-ray through a suitable thickness of aluminium, the lines in question, having a shorter wavelength than the first-order lines, will decrease much less than those in their immediate vicinity.

With increasing pulse rates the pulse height distribution curve is more and more disturbed and therefore the automatic discriminator will be less effective. This is mainly caused by the generation of anomalous high pulses as a consequence of the limited resolving time τ of the preamplifier. By connecting an oscilloscope with the output of the cathode follower the appearance of these piled up pulses is easy to demonstrate when the x-ray intensity increases. The pulse height distribution curves of figure 10, plotted for low and

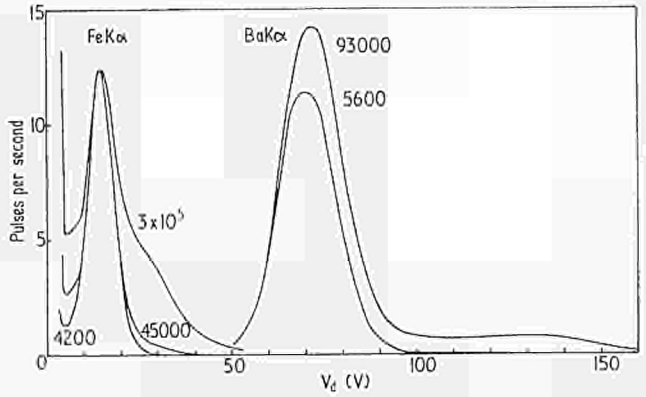

Figure 10. Pulse height distribution curves taken at low and high pulse rates for the lines FeKα (at 20 kv operating voltage) and BaKα (at 50 kv). The scale factor for the lines 4200 and 5600 sec^{-1} is 1/10, for 45000 and 93000 it is 1/100 and for the line 3×10^5 sec^{-1} it is 1/200.

for high pulse rates, illustrate the curve deformation. This deformation obviously decreases the measured pulse rate at the first-order position compared with measurements without discriminator and simultaneously increases the pulse rate at the position of double energy. The first-mentioned property apparently increases τ (approximately by a factor of two, dependent on the channel width); the last-mentioned diminishes considerably the discrimination effect of the nth order spectra as is shown for the element Fe in figure 9. In addition to this effect, high pulse rates displace the tube potentials in the electronic circuits and cause a slow voltage shift of the discriminator threshold, but this effect is less important.

6. Conclusions

It is possible to synchronize the bias voltage and the window width of the pulse height discriminator by means of a function generator using only linear potentiometers. The correct adjustment is carried out electrically and not mechanically. The circuit may be adapted to different reflection orders and also to different analysing crystals. In the present state the device gives linear response within the pulse rate range up to 2×10^4 sec^{-1}. To exceed this limit, the preamplifier must be transformed.

Automatic discrimination has been developed for qualitative mineral analysis and for quantitative geochemical multi-element trace analysis to simplify the interpretation of the spectral diagrams. In particular, routine determination of the K-spectra of Ti, V, Cr, Mn, Co and Ni, and of the L-spectra of Ba and the rare earths, has been speeded up considerably. As rock specimens are already considerably transparent at the wavelength of BaKα, the results obtained from Kα determinations in this range of wavelength are not too accurate. Therefore the possibility of using the L-spectra for routine determination of elements in this range has been a major improvement on previous techniques. It is remarkable that even Ca and K can be determined with the arrangement used in figure 9 (for the last element only the Kβ-line is visible with an LiF crystal). As the x-ray analysis of elements with $Z < 18$ demands a separate and extremely careful specimen preparation (Rose *et al.* 1962 unpublished), it is of interest to include the analysis of Ca and K by the present method. The natural abundance of these two elements of about 1 to 3% in the rocks allows of a serious analysis with the help of the discriminator. In this case practically all elements influencing an average Al_2O_3–SiO_2 rock matrix are detected by the scintillation counter method. This is important for theoretical matrix calculations.

The high sensitivity of the arrangement demands special attention to contamination of the spectra by escape lines, especially when operating voltages higher than 50 kv are used. In all cases, however, the escape lines can be identified by their anomalous behaviour when an absorption foil is used.

As a curiosity it may be observed that additional experiments, using an EDDT analysing crystal, have demonstrated the possibility of detecting elements up to sulphur by means of a scintillation counter (equipped with a Philips 150 AVP photomultiplier operating at $V_h = 850$ volts and without special cooling) associated with our spectrometer (air path ~ 3 cm + 200 μm Be + 1 μm Al + 18 μm mylar). This is very close to the operating limit of a NaI(Tl) scintillator, found by West *et al.* (1951). Of course, in the last-mentioned λ-region the pulse height distribution is too large to allow a serious discrimination to be carried out and in general the detection limit may also be insufficient.† But these results show that a very efficient discrimination can be expected by means of a gas flow proportional counter in the region between the CaKα and the NaKα lines, although the small number of elements do not necessitate an automatic discrimination.

Acknowledgments

We thank the European Atomic Energy Community for enabling us to execute this work and for permission to publish these results.

† Present limit: 2% $min^{1/2}$. With small variations of the previous technique—reducing the air path and the thickness of the Be foil, using a 480 μm collimator and a pentaerythritol analysing crystal—it should be possible to detect 1000 p.p.m. of sulphur in an analysing time of one minute.

References

AXEL, P., 1954, *Rev. Sci. Instrum.*, **25**, 391.

BIRKS, J. B., 1960, *Scintillation Counters*, 3rd edn (London: Pergamon), p. 18.

BLOCHIN, M. A., 1957, *Physik der Röntgenstrahlen* (Berlin: VEB-Verlag Technik), p. 427.

Chem. Weekbl., 1962, **58**, 66.

HEINRICH, K. F. J., 1961, *Advances in X-ray Analysis*, Vol. 4, 1st edn (Ed. W. M. Mueller) (London: Pitman), p. 370.

LANG, A. R., 1954, *German Patent No.* 1023246 (25.8.54).

MEYERHOF, W. E., and WEST, H. I., JR., 1955, *Rev. Sci. Instrum.*, **26**, 1025.

RIGGS, F. B., 1963, *Rev. Sci. Instrum.*, **34**, 312.

WEBER, K., BOUVELLE, G., and MARCHAL, J., 1963, *Rapport EURATOM*, Brussels (Belgium).

WEST, H. I., JR., MEYERHOF, W. E., and HOFSTADTER, R., 1951, *Phys. Rev.*, **81**, 141.

UNWIN BROTHERS LIMITED, WOKING AND LONDON

CDNA00572ENC